Jardim, G. A. M., Silva, T. L., Goulart, M. O. F., de Simone, C. A., Barbosa, J. M. C., Salomão, K., ... da Silva Júnior, E. N. (2017). Rhodium-catalyzed C-H bond activation for the synthesis of quinonoid compounds: Significant Anti-Trypanosoma cruzi activities and electrochemical studies of functionalized quinones. *European Journal of Medicinal Chemistry*, *136*, 406–419. https://doi.org/10.1016/j.ejmech.2017.05.011

Rhodium-Catalyzed C-H Bond Activation for the Synthesis of Quinonoid Compounds: Significant Anti-*Trypanosoma cruzi* Activities and Electrochemical Studies of A-Ring Functionalized Quinones

Guilherme A. M. Jardim,[a] Thaissa L. da Silva,[b] Marilia O. F. Goulart,[b] Carlos A. de Simone,[c] Juliana M. C. Barbosa,[d] Kelly Salomão,[d] Solange L. de Castro,[d] John F. Bower[e] and Eufrânio N. da Silva Júnior[a]*

[a]Institute of Exact Sciences, Department of Chemistry, Federal University of Minas Gerais, CEP 31270-901, Belo Horizonte, MG, Brazil;
[b]Institute of Chemistry and Biotechnology, Federal University of Alagoas, CEP 57072-970, Maceió, AL, Brazil;
[c]Department of Physics and Informatics, Institute of Physics, University of São Paulo, São Carlos, 13560-160, SP, Brazil;
[d]Laboratory of Cellular Biology, IOC, FIOCRUZ, Rio de Janeiro, RJ, 21045-900, Brazil;
[e]School of Chemistry, University of Bristol, Bristol, BS8 1TS, UK.

Corresponding author: E.N. da Silva Júnior: E-mail: eufranio@ufmg.br; Fax: +55 31 34095700; Tel.: +55 31 34095720.

Abstract: Thirty four halogen and selenium-containing quinones, synthesized by rhodium-catalyzed C-H bond activation and palladium-catalyzed cross-coupling reactions, were evaluated against bloodstream trypomastigotes of *T. cruzi*. We have identified nine compounds with IC_{50}/24 h values of less than 2 μM. Electrochemical studies on A-ring functionalized naphthoquinones were also performed aiming to correlate redox properties with trypanocidal activity. For instance, (*E*)-5-styryl-1,4-naphthoquinone **60** and 5,8-diiodo-1,4-naphthoquinone **3**, which are around fifty fold more active than the standard drug benznidazole, are potential derivatives for further investigation. These compounds represent powerful new agents useful in Chagas disease therapy.

Keywords: C-H functionalization, Quinones, Chagas disease, *Trypanosoma cruzi*, Electrochemistry.

1. Introduction

Chagas disease, caused by *Trypanosoma cruzi* (*T. cruzi*), is classified as a neglected tropical disease by the World Health Organization. This disease has high morbidity and mortality rates, affects 5-7 million people and displays a limited response to therapy [1]. It is transmitted to humans by triatomine vectors, blood transfusions, oral and congenital routes and less commonly, by organ transplantation, and laboratory accidents [2]. Chagas disease is characterized by two clinical phases: a short, acute phase defined by patent parasitaemia and a long, progressive chronic phase. The acute phase appears shortly after infection and is frequently asymptomatic. After 2 to 3 months, in most infected individuals, a host/parasite balance is achieved, leading to the chronic phase. Approximately two thirds of infected individuals remain in the indeterminate chronic form, but after 10 to 30 years, the other third will develop a symptomatic chronic disease with digestive and/or cardiac disturbances [3]. Two current major concerns are outbreaks of acute Chagas disease associated with the ingestion of contaminated food [4], and the disease's emergence in non-endemic areas such as North America and Europe, due to the immigration of infected individuals [5].

T. cruzi is a hemoflagellate protozoan and its life cycle involves distinct forms during its passage through vertebrate and invertebrate hosts. The trypomastigote form ingested by the insect differentiates into the proliferative epimastigote form, which, on reaching the posterior intestine of the insect, differentiates into the metacyclic form. The latter, following invasion of vertebrate host cells, undergoes differentiation into the amastigote form, which, after several reproductive cycles, transforms into the trypomastigote form, responsible for the dissemination of the infection.

The current treatment for Chagas disease is restricted to two nitroheterocyclic drugs, benznidazole (Bz) and nifurtimox (Nif), and their efficacy varies according to the phase of the disease, with their effectiveness decreasing with advancement of the infection [6]. The major limitations of these drugs are their limited and variable curative activity in the established chronic form of the disease and their toxic effects, leading to treatment abandonment in several instances [7]. These drawbacks justify the urgent need to identify better drugs to treat chagasic patients. In this context, an intensive research program has focused upon the search for alternative natural, semi-synthetic and synthetic lead compounds [8].

Over the last few years, our group has dedicated efforts to the synthesis and identification of novel naphthoquinoidal compounds with potent antiparasitic activity [9]. In this context, we have modified the "redox centre" A- and C-rings of lapachones with the aim of preparing new bioactive compounds [9c]. For instance, a simple redox centre modification of β-lapachone led to a phenazine derivative with trypanocidal activity about two and six times higher than benznidazole and the original quinone, respectively [10]. Intrinsically related to this strategy, we have demonstrated that appendage of a triazole group to the C-ring of β-lapachone affords a derivative four times more active against the parasite than the naphthoquinoidal precursor [11]. Recently, Lim and co-workers [12] described the synthesis and evaluation of A-ring modified lapachones, which show activity against cancer cells (Scheme 1A); this study is of direct relevance to the strategies outlined herein.

Salomão and co-workers have reported the trypanocidal activity of C-2 and C-5 substituted naphthoquinones, as well as evidence for their mode of action [13]. As shown in Scheme 1B, in assays performed in the absence of blood and with incubation at 37°C several compounds presented IC_{50} values of < 2 μM against *T. cruzi*. For instance, further assays with 5-acetoxy-1,4-naphthoquinone (IC_{50} = 0.16 μM) revealed activity against the proliferative forms of *T. cruzi*, intracellular amastigotes and epimastigotes. In experiments with this latter parasite form, this compound led to mitochondrial swelling, vacuolization, and flagellar blebbing, as well as a remarkable decrease in the mitochondrial membrane potential and a discrete increase of ROS production. Such redox dependent effects are likely reliant on the acetyl group facilitating quinone reduction, as previously demonstrated by electrochemical analysis [13b]. These results show that A-ring substituted naphthoquinones can kill *T. cruzi* and highlight the importance of synthesizing and evaluating new quinoidal compounds against parasites.

Recently, our group has embarked on a research program aimed at addressing unmet synthetic challenges related to quinone modification. For instance, we have demonstrated that chiral squaramide catalyzed reaction of lawsone with Morita-Baylis-Hillman acetates of nitroalkenes leads to the asymmetric formation of pyranonaphthoquinones [14]. We have also developed C-H activation-based processes that achieve challenging bond formations and enable late stage functionalization of complex systems [15]. For example, we reported recently a method for the A-ring functionalization of naphthoquinones that is reliant on a rhodium-catalyzed C-5 selective C-H iodination reaction [16]. In this report, we outline the C-H functionalization enabled

synthesis of 30 quinoidal derivatives and their evaluation against *T. cruzi*. Four compounds were also prepared by C-C bond forming reactions achieved via palladium catalysis. Since the biological activity of quinones is intrinsically related to the quinoidal redox centre, we also describe the electrochemical behavior of nine representative compounds.

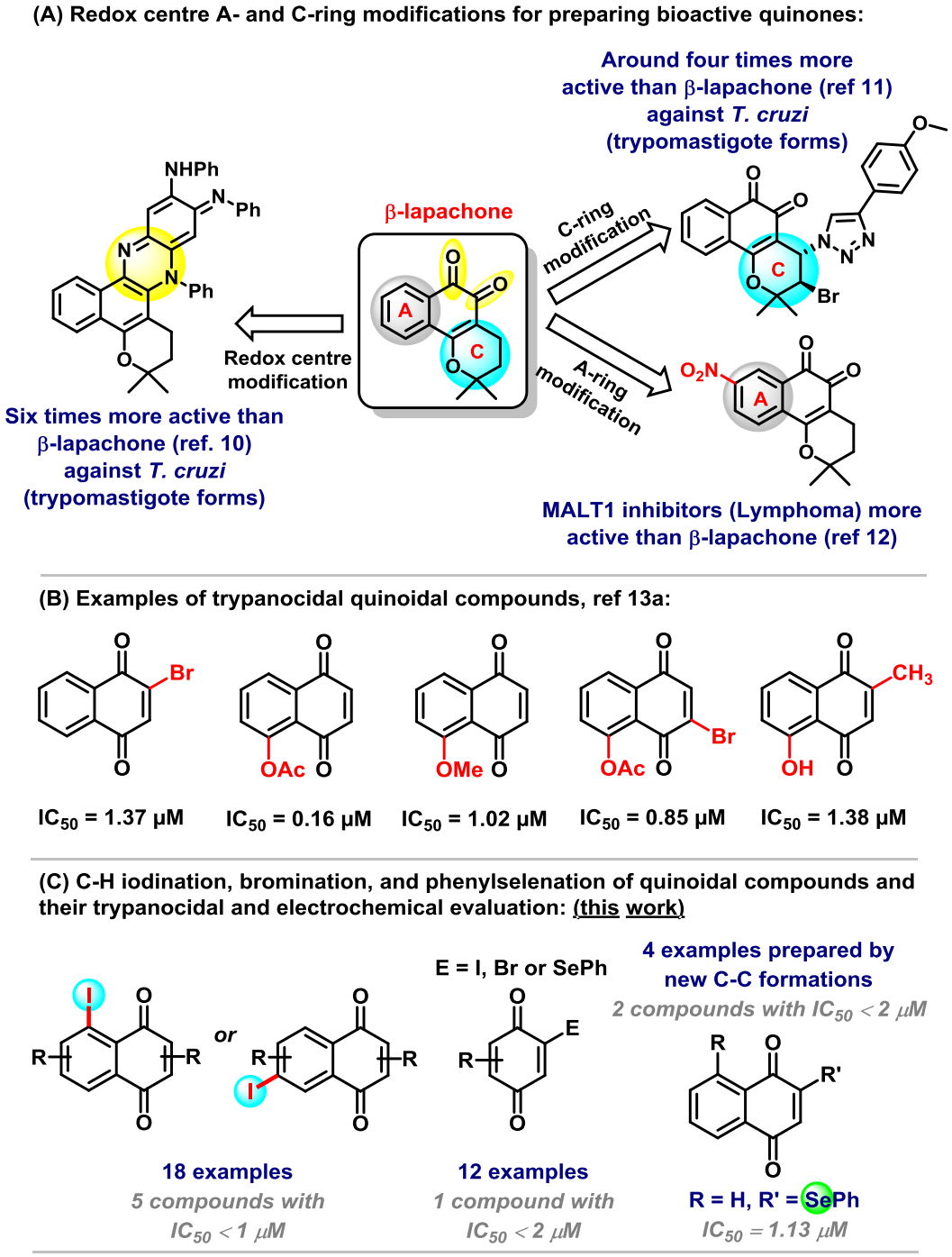

Scheme 1. Overview.

2. Results and Discussion

2.1 Chemistry

Naphthoquinone derivatives were the first class of compounds targeted for preparation. A-ring modifications were performed utilizing a carbonyl directed Rh-catalyzed C-H bond activation protocol reported recently by our group [16]; this methodology allowed C-5 selective iodination of several 1,4-naphthoquinones. In the simplest case, using 1,4-naphthoquinone (**1**) as substrate, the synthesis of mono-iodinated product **2** occurred in 69% yield, accompanied by a 5% yield of bis-iodinated by-product **3** (Scheme 1). For the purpose of clarity the numbering system shown in Scheme 1 is used during further discussion.

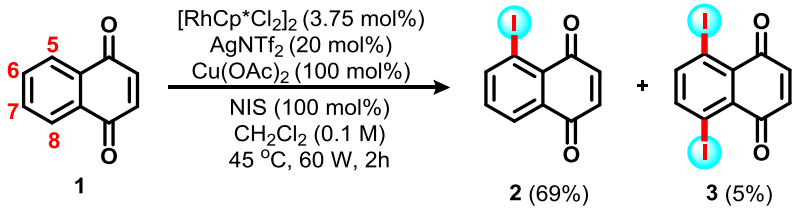

Scheme 1. Iodinated naphthoquinoidal derivatives **2** and **3**.

Iodinated naphthoquinones containing electron donating and withdrawing groups were selected for subsequent biological evaluation. The use of hydroxyl A-ring-substituted substrates (e.g. **4**) changed the regioselectivity of iodination to afford **5**, where functionalization had occurred *ortho* to the hydroxyl group (C7) rather than at C5; this demonstrates that the carbonyl-directed pathway can be overridden by strong donor substituents. Control experiments showed that in the absence of the Rh-catalyst only traces of product were observed. Use of 250 mol% NIS enabled subsequent C5 iodination of **5** to provide **6** in 82% yield. Reaction of plumbagin **7** with 100 mol% NIS provided C7 iodination product **8** in 85% yield. Juglone (**4**) and plumbagin (**7**) were reacted with iodomethane and Ag_2O in $CHCl_3$ to afford **9** and **10** in 73% and 78% yield, respectively [17]. Rh-catalyzed C-H iodination of these substrates gave **11** and **12** in excellent yields. To prepare compounds containing methoxy groups in different A-ring positions, derivatives **5** and **8** were also methylated to afford **13** and **14** in 91% and 92% yield, respectively (Scheme 2).

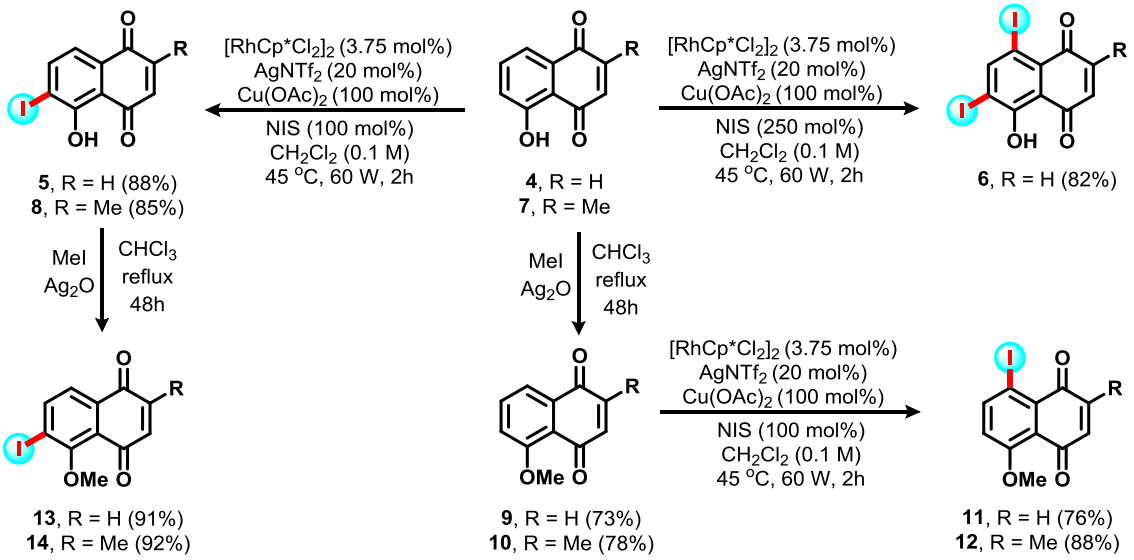

Scheme 2. Iodinated A-ring substituted naphthoquinones **5**, **6**, **8** and **11**-**14**.

Other substrates containing methoxy groups were obtained in good yields by oxidation of tetralones **15** and **16** with 2-iodo-benzoic acid and Oxone (substrates **17** and **18**) [18]. When the C-H iodination methodology was applied to these substrates derivatives **19** and **20** were generated in good to excellent yields. The regioselectivity observed for the iodination of **19** is suggestive of secondary coordination of the methoxy group to the Rh-center, thereby facilitating functionalization at the most hindered A-ring position (Scheme 3). Consistent with this assertion, iodination of compound **21**, in which the methoxy group of **19** has been replaced by a methyl substituent, occurred selectively at the less hindered position to generate **22** in 63% yield (Scheme 4).

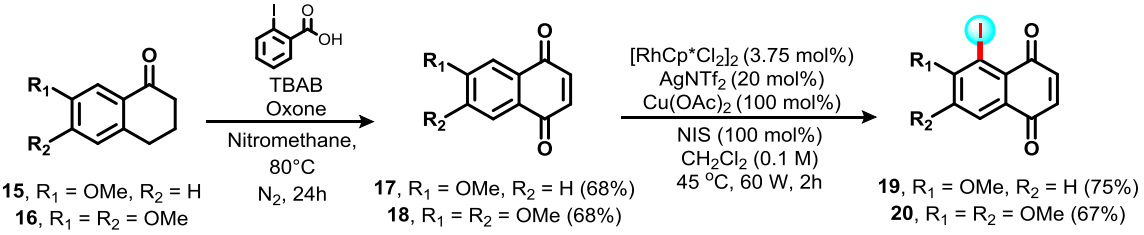

Scheme 3. Preparation of iodinated derivatives **19** and **20** from tetralones.

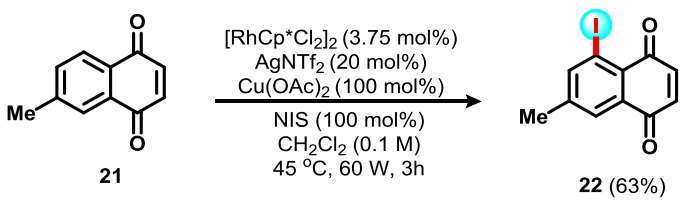

Scheme 4. Synthesis of iodinated quinone **22**.

In order to investigate the effects of other electron donating groups, iodination of **24**, which contains an amino group, was pursued. Consistent with hydroxy containing systems **4** and **7**, functionalization occurred at C-7 to afford **25** in 41% yield and with high selectivity. On other hand, iodination of **27**, which contains an electron withdrawing ester at C-8, was selective for C-5, affording derivative **28** in 57% yield (Scheme 5). Note that Ivashkina and co-workers [19] have described the synthesis of **25** using I_2-HIO_3 but the product was obtained as mixture of C-5 and C-7 iodinated products.

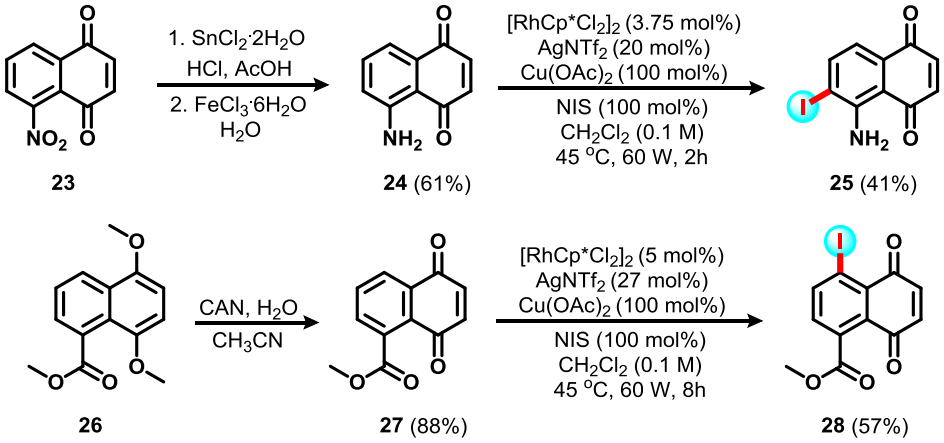

Scheme 5. Iodinated compounds **25** and **28** prepared from **23** and **26**.

Electron deficient naphthoquinones were also used as substrates, affording the targets in moderate to good yields. Interestingly, unsymmetrical substrate **29** delivered **30** (59% yield) as the sole product, indicating that the bromine substituent controls the relative directing ability of the two carbonyl groups for the metalation event (Scheme 6).

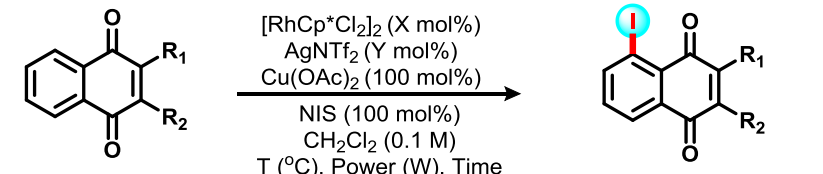

[a] X = 3.75, Y = 20, T = 45 °C, Power = 60 W, Time = 2h
[b] X = 5, Y = 27, T = 65 °C, Power = 75 W, Time = 4h
[c] X = 5, Y = 27, T = 45 °C, Power = 60 W, Time = 8h

Scheme 6. Iodinated naphthoquinoidal derivatives **30**, **32** and **34**.

We also sought to investigate the biological effects of substituents on other quinone-based systems. The evaluation of heteroatom substituted benzoquinoidal compounds as potential trypanocidal agents was particularly attractive because these can be accessed directly by our reported C-H functionalization protocol (Scheme 3) [20]. Rh-catalyzed reaction of 1,4-benzoquinone **35** with 1,3-diiodo-5,5-dimethylhydantoin (DIH) yielded derivative **36** in 95% yield. Exchanging the electrophile source to 1,3-dibromo-5,5-dimethylhydantoin (DBH) afforded **37** in 82% yield. C-H phenylselenation processes were also investigated. Reaction of **35** with 150 mol % *N*-(phenylseleno)phthalimide afforded a mixture of target **38** and bis-functionalization product **39**. However, it was found that by using only 100 mol% *N*-(phenylseleno)phthalimide, **38** could be obtained in good yield and with high selectivity over **39** (4.5:1 selectivity). The latter compound could be accessed exclusively in 74% yield by using an excess (250 mol %) of *N*-(phenylseleno)phthalimide (Scheme 7).

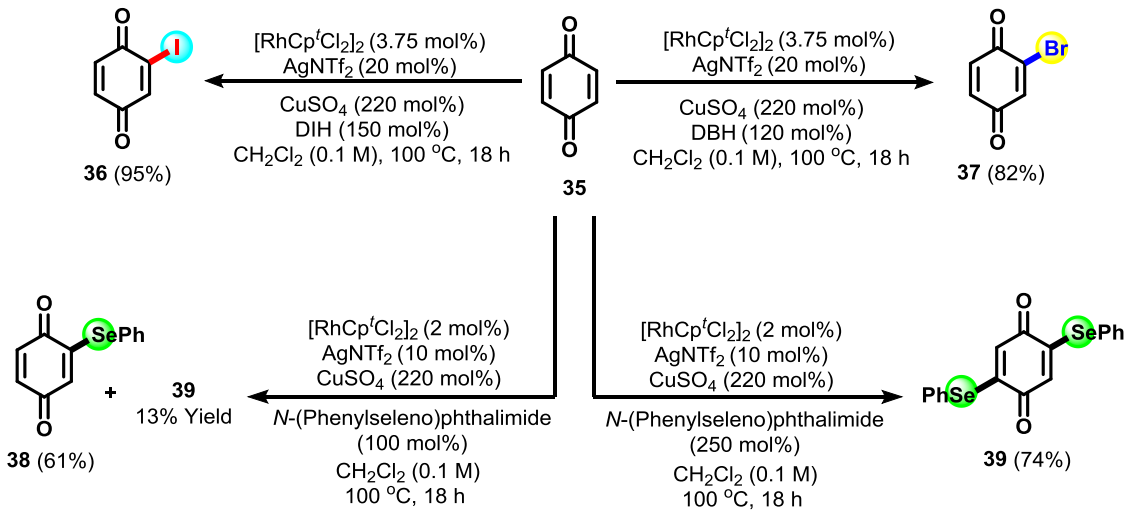

Scheme 7. Chalcogenated **38** and **39** and iodinated derivatives **35** and **36**.

Rh-catalyzed iodination of alkyl-substituted system **40** afforded target **41** in 66% yield and good regioselectivity. Here, iodination occurs at the site remote to the bulky *tert*-butyl group. A similar result was obtained for bromination of **40** to deliver **42** in 57% yield (Scheme 8).

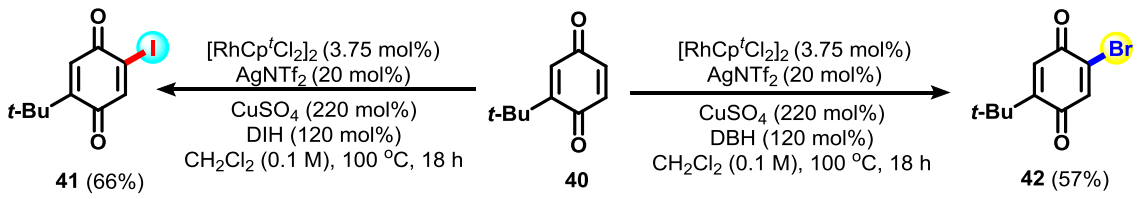

Scheme 8. Synthesis of iodinated quinone **41** and brominated one **42** from **40**.

The metal-catalyzed protocol was also applied to benzoquinone **46**, containing two adjacent methyl groups, and this afforded **49** in 81% yield. Interestingly, attempted bromination of **46** lead to degradation. For benzoquinone **47**, which contains an electron-donating methoxy-group, iodination occurred at the most electron rich position to afford **50** in 91% yield. Bis-iodination of bis-methoxy system **48** was achieved in high yield by using an excess of DIH to generate **51** in 76% yield (Scheme 9).

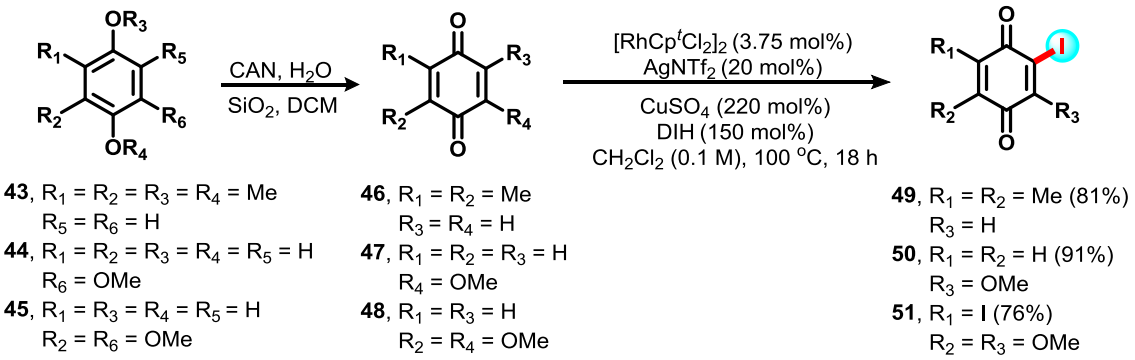

Scheme 9. Iodinated quinoidal derivatives.

Systems possessing electron-withdrawing substituents proved to be more challenging; for example, electron deficient substrate **52** reacted smoothly with DIH to provide **53** in 56% yield. Bromination of **52** provided **54** in only 45% yield (Scheme 10).

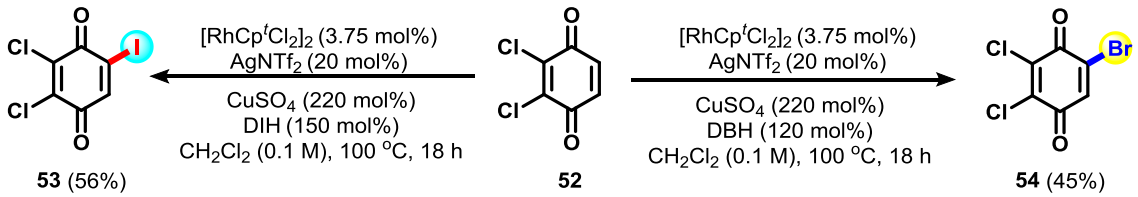

Scheme 10. Preparation of iodinated derivative **53** and brominated **54** from electron deficient compound **52**.

As outlined in Scheme 11, application of the C-H functionalization conditions to 1,4-naphthoquinone **1** provided derivatives **55** and **56** in excellent yields and high selectivity. The use of $[RhCp^tCl_2]_2$ in combination with $CuSO_4$ was required to achieve C-2 rather than C-5 selectivity (cf. Scheme 2). This aspect is notable because site-

selective C-H functionalization of naphthoquinones (C-2 versus C-5) is achieved under catalyst control (cf. Scheme 1).

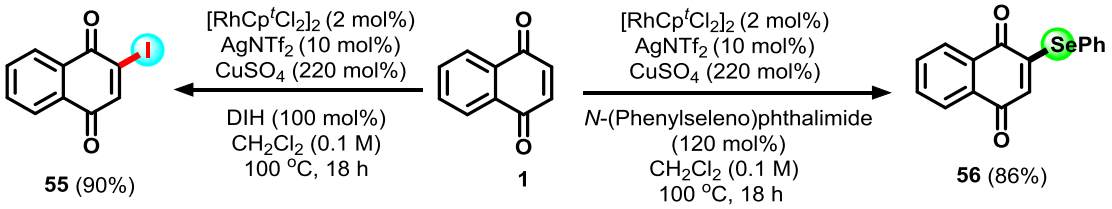

Scheme 11. C-2 substituted naphthoquinones **55** and **56**.

Because iodination of 1,4-naphthoquinone was readily achieved, subsequent palladium-catalyzed C-C bond forming derivatizations also became accessible (Scheme 12), thereby providing an avenue for the synthesis of different classes of hybrid quinonoid-based compounds. Under highly optimized conditions,[21] Stille coupling of **2** afforded **57** in 75% yield. Heck alkenylations [22] of **2** with ethyl acrylate and styrene proceeded smoothly to provide **58** and **59**, respectively. Several Sonogashira cross-coupling protocols were evaluated without success. To solve this problem, a previously reported procedure [23] was employed, wherein reaction of **2** with an alkynyl-copper(I) reagent provided Sonogashira-like product **60** in 64% yield.

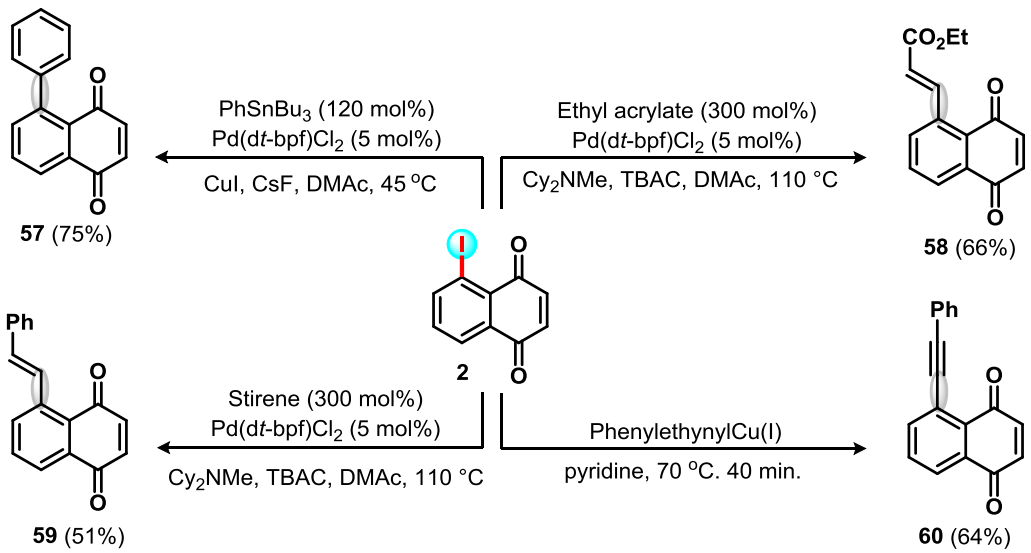

Scheme 12. Derivatization of **2** via palladium catalyzed C-C bond formatting reactions.

The structures of novel compounds **5**, **6**, **8**, **13**, **14**, **25, 49** and **59** were determined by ^{1}H, ^{13}C and 2D NMR analysis in combination with either electrospray ionization or

electronic impact mass spectrometry. Additionally, compounds **5**, **6** and **51** were analyzed by single crystal X-ray diffraction, as summarized below.

2.2. X-ray analysis

Compound **5** crystallizes in space group $P2_1/c$ with four independent molecules in the asymmetric unit where two of them are superimposed with occupational disorder on some atoms. For clarity, only one molecule is shown in Figure 1. The molecule is perfectly planar (r.m.s. deviation = 0.0029 A° for 14 non-hydrogen atoms). In the packing of the crystal, five C-H---O type interactions and three O-H---I type interactions link the molecules, forming chains that extend along the [b] axis and parallel to (4 0 4) plane.

Compound **6** crystallizes in space group $P2_1/n$ with two molecules in the asymmetric unit. For clarity, only one molecule is shown in Figure 1. There are no significant conformational differences between them. The molecule is almost planar (r.m.s. deviation = 0.0051 A° for I3 non-hydrogen atoms) except the I1 and I2 atoms that are out of the mean plane of the rings with deviations of -0.179(3) and 0.137(2) A° respectively. In the crystal, molecules are linked by weak interactions C2-H2---O3 [d(H2⋯O3) = 2.56(2) Å, \(C2-H2⋯O3) = 125(4)°], C18-H18---O2 [d(H18⋯O2) = 2.42(2) Å, \(C18-H18⋯O2) = 170(3)°] and O-H---I [d(H⋯I) = 3.53(2)Å] forming chains parallel to the (3 -3 -3) and (3 3 -3) planes.

Finally, compound **51** crystallizes in space group Pnma. The molecule is symmetric where the asymmetric units are C1, C2, C3, C4, C5 I1, O1, O2 and O3. The I1, O1 and O3 atoms deviate from the mean plane of the ring by -0.154(2), -0.111(2) and -0.388(3) A°, respectively. The C2-C3-O2-C5 torsion angle of the methoxy group is -158.2(2)°. In the crystal, the molecules are linked by I---O (methoxy group) teractions [d = 3.383(2) A°] resulting in a highly symmetrical arrangement that extends along the [a] axis.

An Ortep-3 diagram of each molecule is shown in Figure 1 and Table 1 lists the main crystallographic data for **5**, **6** and **51**. Packing diagrams for all compounds are provided in the Supporting Information File.

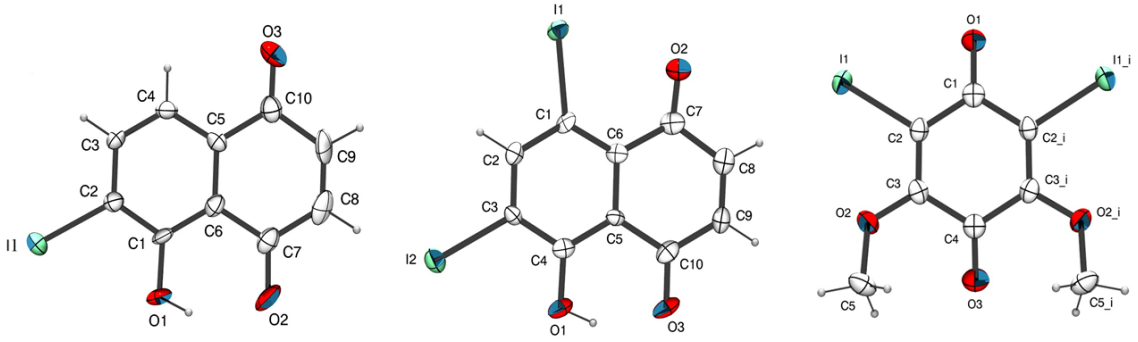

Figure 1. A projection ORTEP-3 of **5**, **6** and **51**, showing the atom-numbering and displacement ellipsoids at the 50% probability level.

Table 1. Crystal data and structure refinement for compounds **5**, **6** and **51**.

Identification code	Compound **5**		Compound **6**		Compound **51**	
Empirical formula	$C_{10}H_5IO_3$		$C_{10}H_4I_2O_3$		$C_8H_6I_2O_4$	
Formula weight	315.5		425.9		419.9	
Temperature	293(2) K		293(2) K		293(2) K	
Wavelength	0.71073 Å		0.71073 Å		0.71073 Å	
Crystal system	monoclinic		monoclinic		orthorhombic	
Space group	$P2_1/c$		$P2_1/n$		Pnma	
Unit cell dimensions	a = 7.7911(6) Å	α = 90°	a = 8.2431(2) Å	α = 90°	a = 9.5066 (4) Å	α = 90°
	b = 27.0192(4) Å	β = 93.1(5)°	b = 15.1653(4) Å	β = 92.95(2)°	b = 17.3636 (8)Å	β = 90°
	c = 13.5802(12) Å	γ = 90°	c = 16.8525(5) Å	γ = 90°	c = 6.3177 (2) Å	γ = 90°
Volume	2854.8(9) $Å^3$		2103.9(2) $Å^3$		1698.7 (2) $Å^3$	
Z	4		8		4	
Density (calculated)	2.17 Mg/m^3		2.69 Mg/m^3		2.67 Mg/m^3	
Absorption coefficient	3.6 mm^{-1}		5.9 mm^{-1}		6.01mm^{-1}	
F(000)	1756		1552		768	
Theta range for data collection	1.7 to 27.9°		1.8 to 27.1°		2.3 to 27.9°	
Index ranges	-9≤h≤10, -35≤k≤35, -13≤l≤17		-10≤h≤10, -19≤k≤19, -21≤l≤21		−12≤h≤12, −22≤k≤22, −8≤l≤8	
Collected Reflections	25651		16620		8822	
Absorption correction	none		none		none	
Refinement method	Full-matrix least-squares on F^2		Full-matrix least-squares on F^2		Full-matrix least-squares on F^2	
Data / restraints / parameters	5975 / 0 / 448		3421 / 0 / 273		1241 /0 / 71	
Goodness-of-fit on F^2	1.34		1.004		1.21	
Final R indices [I>2sigma(I)]	R1 = 0.074, wR2 = 0.15		R1 = 0.037, wR2 = 0.062		R1 = 0.014, wR2 = 0.034	
R indices (all data)	R1 = 0.084, wR2 = 0.152		R1 = 0.064, wR2 = 0.069		R1 = 0.015, wR2 = 0.034	

2.3. Biological Studies

The potential of simple structural modifications for increasing antiparasitic activity of naphthoquinones is shown in Scheme 6. Juglone, a naturally occurring naphthoquinone, displays an IC_{50}/24 h value of 6.51 µM [13a]. We have previously reported that the addition of methyl or bromine groups to C-5 and/or C-7 leads to new naphthoquinones that are 4.7 and 5.2 times more active against *T. cruzi* than juglone, respectively. Remarkably, a 40 fold increase in activity is observed for the O-acetoxy derivative of juglone [13a] (Scheme 13).

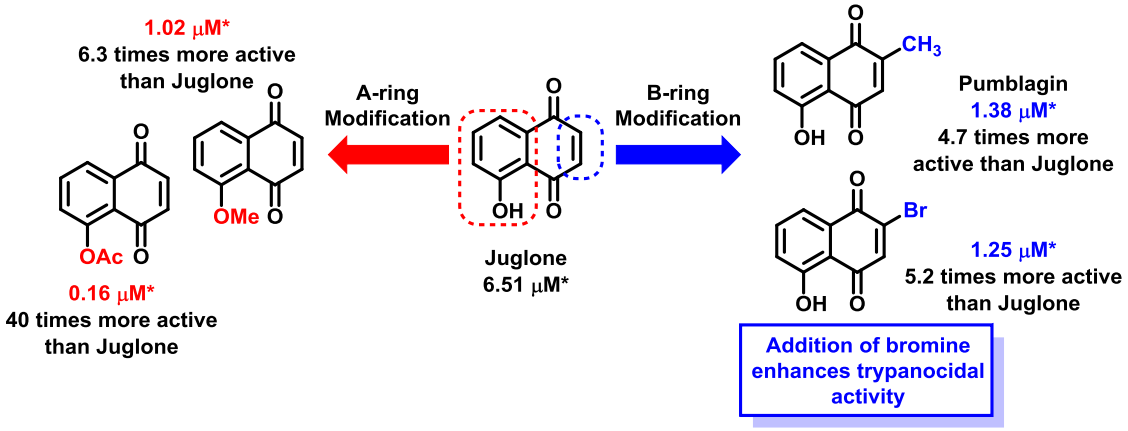

Scheme 13. Simple modifications in juglone leading to compounds with potent trypanocidal activity. *IC_{50}/24 h values for the lytic activity on bloodstream trypomastigotes.

Considering these previous results and recent reports in the literature [24,25], we have accomplished modifications to the quinoidal system leading to A-, B-, or A- and B-ring substituted compounds, and these were assayed against *T. cruzi*. Note that direct functionalization by rhodium-catalyzed C-H bond activation allows the efficient and fast preparation of potent quinoidal compounds, as shown in Scheme 14.

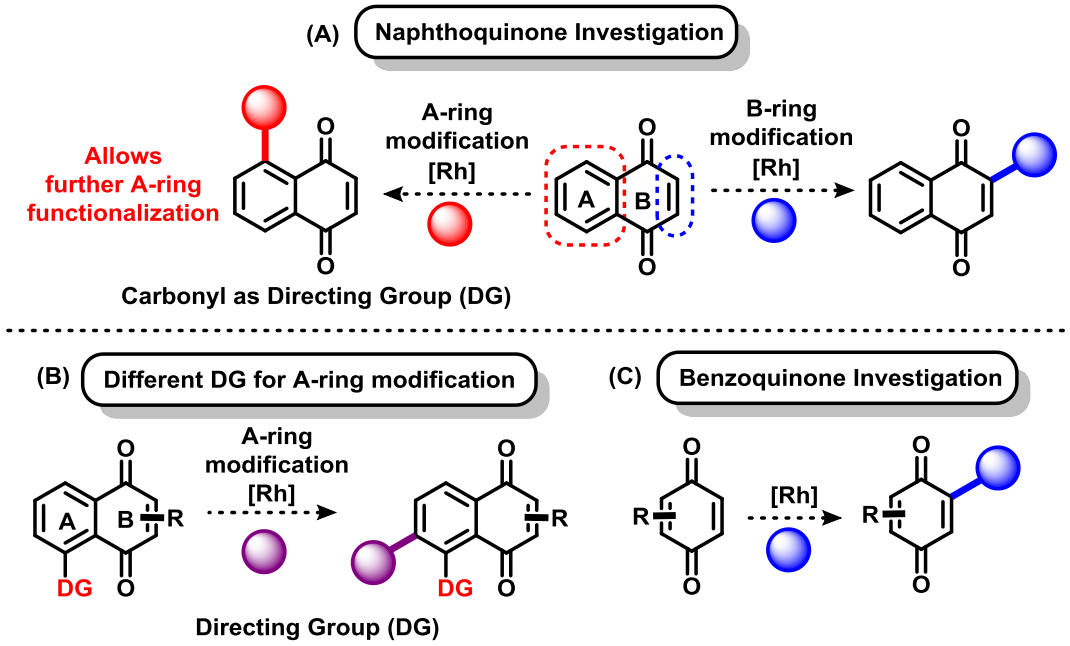

Scheme 14. Strategies for the synthesis of novel trypanocidal naphthoquinones and benzoquinones.

Compounds were evaluated against bloodstream forms of *T. cruzi* (IC_{50}/24 h) and mammalian cells (LC_{50}/24 h), allowing the determination of the selectivity index (SI) derived from the ratio of LC_{50}/IC_{50} (Table 2). From these 34 compounds, 22 are more active than benznidazole, the reference drug (IC_{50}/24 h = 9.68 ± 2.35 µM), with **2**, **3**, **13**, **14**, **19**, **20**, **2l**, **22**, **25**, **28**, **51**, **55**, **56**, **57** and **59** exhibiting IC_{50}/24h values lower than 2 µM, with an SI of between 7.5 and 62.5.

Compounds **2** and **3** show significant activity against the parasite with IC_{50} values of 0.59 and 0.22 µM, respectively, low toxicity for the mammalian cell, and an SI higher than 19. Diiodinated naphthoquinone **3** was obtained as a by-product (vide supra) in poor yield (5%) and further optimization of its preparation will be necessary. In general, the presence of iodine and electron donating groups on the A-ring increases activity against *T. cruzi* and highlights the importance of our Rh-catalyzed C-H iodination methodology. Compounds **22** (IC_{50} = 0.49 µM, SI 24.7) and **25** (IC_{50} = 0.56 µM, SI 23.4), which combine either a methyl or amino group with an iodine substituent, show important activity, being around 20 times more active than benznidazole. As such, **22** and **25** are prototypes that warrant further study. Conversely, the presence of electron withdrawing groups on A-ring and, in some cases, a methyl group leads to decreased activity against *T. cruzi* [**34** (7.26/SI 3.8), **12** (7.57/SI 6.9) and **11** (4.06/SI 6.1)].

Certain benzoquinones also show interesting trypanocidal activity, with an IC_{50} value of less than 2 µM determined for compound **51**. This compound is easily obtained from commercially available benzoquinone in just one-step. C-2 functionalization may be a good general strategy for preparing bioactive compounds, since naphthoquinones substituted at C-2 with iodine (**5** IC_{50} = 1.79 µM, SI 8.2) and selenium (**56**, IC_{50} = 1.13 µM, SI 11.2) were 5.4 and 8.5 times more active than benznidazole, respectively.

Finally, the most active compound (*E*)-5-styryl-1,4-naphthoquinone **59** was prepared in two steps and is described here for the first time. The synthesis of **59** requires C-5 iodinated compound **2**, which is prepared by Rh-catalyzed C-H functionalization. The C-I bond then enables Pd-catalyzed alkenylation with styrene to afford **59**. This compound, with an IC_{50}/24h = 0.19 µM, is fifty fold more active than benznidazole, with an SI of 62.5. Although the studies described here are preliminary, it is worth noting that the combination of a practical synthetic route, high *in vitro* trypanocidal activity and low toxicity to mammalian cells, makes **59** a very attractive hybrid quinone in the search for better trypanocides.

Table 2. Activity of synthetic derivatives against bloodstream trypomastigotes of *T. cruzi* (Y strain) at 37 °C, cytotoxicity to mammalian cells and Selectivity Index (SI).

Compd	IC_{50}/24h (µM)	LC_{50}/24h (µM)	SI
2	0.59 ± 0.08	11.49 ± 0.54	19.5
3	0.22 ± 0.07	12.93 ± 1.43	28.8
5	42.0 ± 3.11	> 100	> 4.6
6	24.8 ± 4.49	> 100	> 5.1
8	0.99 ± 0.12	15.72 ± 3.49	15.8
11	3.54 ± 0.71	13.59 ± 0.79	3.8
12	7.57 ± 0.56	51.88 ± 10.42	6.9
13	1.35 ± 0.43	13.27 ± 1.73	9.8
14	4.06 ± 0.47	24.67 ± 6.51	6.1
19	1.17 ± 0.23	14.19 ± 3.21	12.1
20	1.62 ± 0.34	12.16 ± 0.16	7.5
22	0.49 ± 0.04	12.09 ± 0.24	24.7
25	0.56 ± 0.05	13.12 ± 1.16	23.4
28	1.61 ± 0.44	13.94 ± 0.21	8.7
30	1.38 ± 0.57	12.15 ± 0.15	8.8
32	2.25 ± 0.48	11.82 ± 0.37	5.3
34	7.26 ± 1.41	27.83 ± 5.17	3.8
36	60.61 ± 6.86	86.02 ± 2.99	1.4
37	21.54 ± 5.83	34.35 ± 2.46	1.6
38	15.95 ± 3.52	13.78 ± 4.37	0.86
39	83.42 ± 9.08	> 100	> 1.2
41	12.77 ± 1.61	35.93 ± 4.92	2.8
42	14.09 ± 2.32	42.30 ± 4.67	3.0

49	10.07 ± 3.26	15.40 ± 3.87	1.5
50	23.95 ± 7.08	32.62 ± 9.71	1.4
51	1.94 ± 0.51	27.71 ± 1.22	1.3
53	26.99 ± 4.30	> 100	> 4.7
54	15.40 ± 1.34	> 100	> 6.5
55	1.79 ± 0.37	14.72 ± 2.68	8.2
56	1.13 ± 0.22	12.67 ± 0.70	11.2
57	1.24 ± 0.31	12.67 ± 0.10	10.2
58	6.03 ± 1.19	12.65 ± 0.26	2.1
59	0.19 ± 0.08	11.87 ± 0.43	62.5
60	2.20 ± 0.33	12.49 ± 0.23	5.7

2.4. Electrochemistry Aspects

Electrochemistry is a useful tool for the design, development and characterization of redox-selective molecules and can provide information on their mechanism of action [26]. Motivated by this approach, we have successfully described the combined use of electrochemistry and biological evaluation to provide insights about the mechanism of action of 3-arylamino lapachone [27], as well as selenium [28] and triazole substituted [29] quinones. The ever-increasing interest in biologically active quinones has resulted in new strategies to decrease toxicity, modulate activity, and direct the compound to the target [30]. As such, it is pertinent to continue to explore their synthesis, biological activities and redox mechanisms through a combined theoretical and experimental approach.

Most quinones, including intermediary and reduced forms, exist inside hydrophobic cell membranes. Consequently, dimethylformamide (DMF) was chosen as an aprotic organic solvent for electrochemical studies, because it can mimic the nonpolar environment in the cell, where lipid peroxidation, one of the causes of membrane fragmentation, normally occurs [24]. We have studied the electrochemical properties of nine quinones. These compounds were selected based on their trypanocidal activity; both active and inactive variants have been studied to enable an understanding of the main qualitative features associated with activity.

As observed in Figure 2, in general there are two reducible systems (the quinone itself and the aryl iodide bond). The electrochemistry of quinones [31] and halogenated compounds, mainly aromatic ones (ArX), has been thoroughly investigated [32] on several electrodes. For quinones, in aprotic medium, general equations 1 to 3 are expected and the quinone/semiquinone/hydroquinone ($Q/SQ^{\bullet -}/H_2Q$) triad is an important component of many redox systems in biology [24,26].

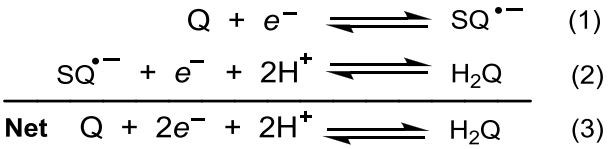

For halides, bi-electronic uptake in aprotic solvents causes rupture of the C-X bond, by either a concerted (Eq. (4)) or stepwise mechanism (Eqs. (5) and (6)), followed by reduction of the ensuing radical (Eq. (7)) to an anion. The latter is usually protonated by residual water to the respective C-H bond [30].

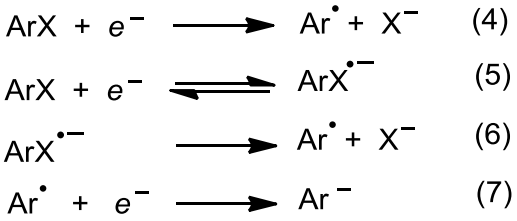

The electrochemistry of iodinated quinones where the halogen is directly attached to the aromatic ring is less widely reported. In the present case, the reduction process of nine iodinated 1,4-naphthoquinones (1,4-NQ), **2**, **3**, **5**, **6**, **11**, **19**, **20**, **22** and **55** was investigated on glassy carbon electrode (GCE), in anhydrous DMF with 0.1 M $TBAPF_6$ as the supporting electrolyte and electrochemical data were compared to trypanocidal activity. A detailed description of the voltammetric behavior of these novel compounds is out of the scope of the present paper. Here we will only consider some features relevant to the discussion of the correlation of redox potentials with trypanocidal activity. Several of the iodo-naphthoquinones analysed have additional A-ring substituents (-OH, $-OCH_3$, and $-CH_3$ groups) and two of them are bis-iodinated (**3** and **6**). All possess an aryl-iodide bond, except **56**, which carries a vinyl iodide. Data on the main reduction peaks, with an emphasis to the first reduction step, Epc_1, appear in Table 2.

Table 3. Major electrochemical parameters of the iodinated quinones (c = 1 mmol L^{-1}), using cyclic voltammetry, on GCE, in DMF/$TBAPF_6$, 0.1 mol L^{-1}, ν = 100 mV s^{-1}.

Compound	Epc_1 (V)	Epc_2 (V)	Epc_3 (V)	Epa'_1 (V)	Epa_1 (V)	Epa'_2 (V)	Epa_2 (V)
2	-0.535	-1.212	-2.198	-	-0.470	-	-1.105

3	-0.521	-1.514	-1.759	-	-0.414	-	-1.129
5	-0.244	-0.903	-	-	-0.148	-	-0.779
6	-0.216	-0.912	-2.057	-	-0.111	-	-0.741
11	-0.625	-1.181	-2.346		-0.550		-1.052
19	-0.616	-1.312	-	-	-0.534	-	-1.175
20	-0.593	-1.314	-	-	-0.514	-	-1.146
22	-0.560	-1.223	-2.242	-	-0.493	-	-1.119
55	-0.413	-1.152	-2.880	-0.517	-0.330	-1.204	-1.044

Considering the ease of the reduction related to Epc_1 (Figure 2), the compounds can be ranked as shown below. Less negative potentials indicate higher electrophilicity: **6** > **5** > **55** > **3** > **2** > **22** >**20** > **19** > **11** (Figure 2).

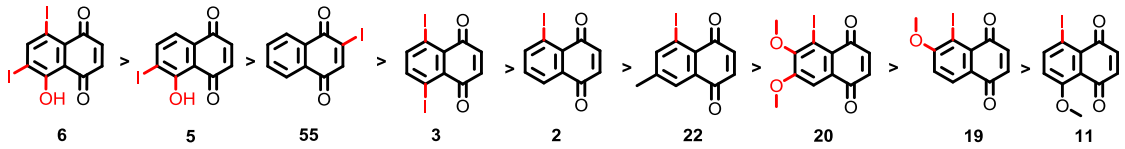

Figure 2. Structures of the naphthoquinones ranked according to data obtained through electrochemical studies

The CV profiles (Figure 2) and structural similarities allow the classification of the compounds into three main electrochemical classes.

The first class contains only one compound, **55**, and is important as it allows comparison of the reduction of aromatic *vs*. vinylic C-I bonds. Aromatic variants suffer much easier reduction (see Epc_3), while the ease of reduction of the quinone moiety is influenced by the electron withdrawing halogen at C2, being reduced at more positive potentials (-0.413 V) than similar C5-iodinated compound **2** (-0.535 V, see table 3).

The second class comprises compounds with substituents that can hydrogen bond (**5** and **6**). This feature results in easier reduction, presumably due to stabilization of the semiquinone (Eq. 1) through hydrogen-bonding. Reduction potentials for **5** and **6** are -0.216 V and -0.244 V, respectively; these values are much more positive than for all the other quinones. The electrochemical reduction of the C-I, leading to bond cleavage (Eqs. 4-7) occurs at highly negative potentials (Epc_3, Table 2).

The third class of compounds, **2**, **3**, **22**, **19**, **11** and **20**, has a different electrochemical profile. The first waves for all of them are related to the generation of the semiquinone (Eq. 1). With one exception, **22**, all of them present an enhanced current at

the level of the second reduction wave ($Ipc_2/Ipc_1 > 1$), with loss of reversibility (Ipa/Ipc < 1). This is related to the reduction of the semiquinone together with the reduction of the C-I bonding. In the case of **3**, where the current (Ipc2) is the highest, the cleavage of both C-I bonds is expected [30] and observed.

Comparison of the Epc1 values with trypanocidal activity reveals a trend, with the two more electrophilic quinones (**5** and **6**) being less active than the others. As quinones are pro-drugs that need to be activated, being so easily reduced, it is possible that **5** and **6** suffer reduction fast, before reaching the biological target, leading, thus, to inactivity.

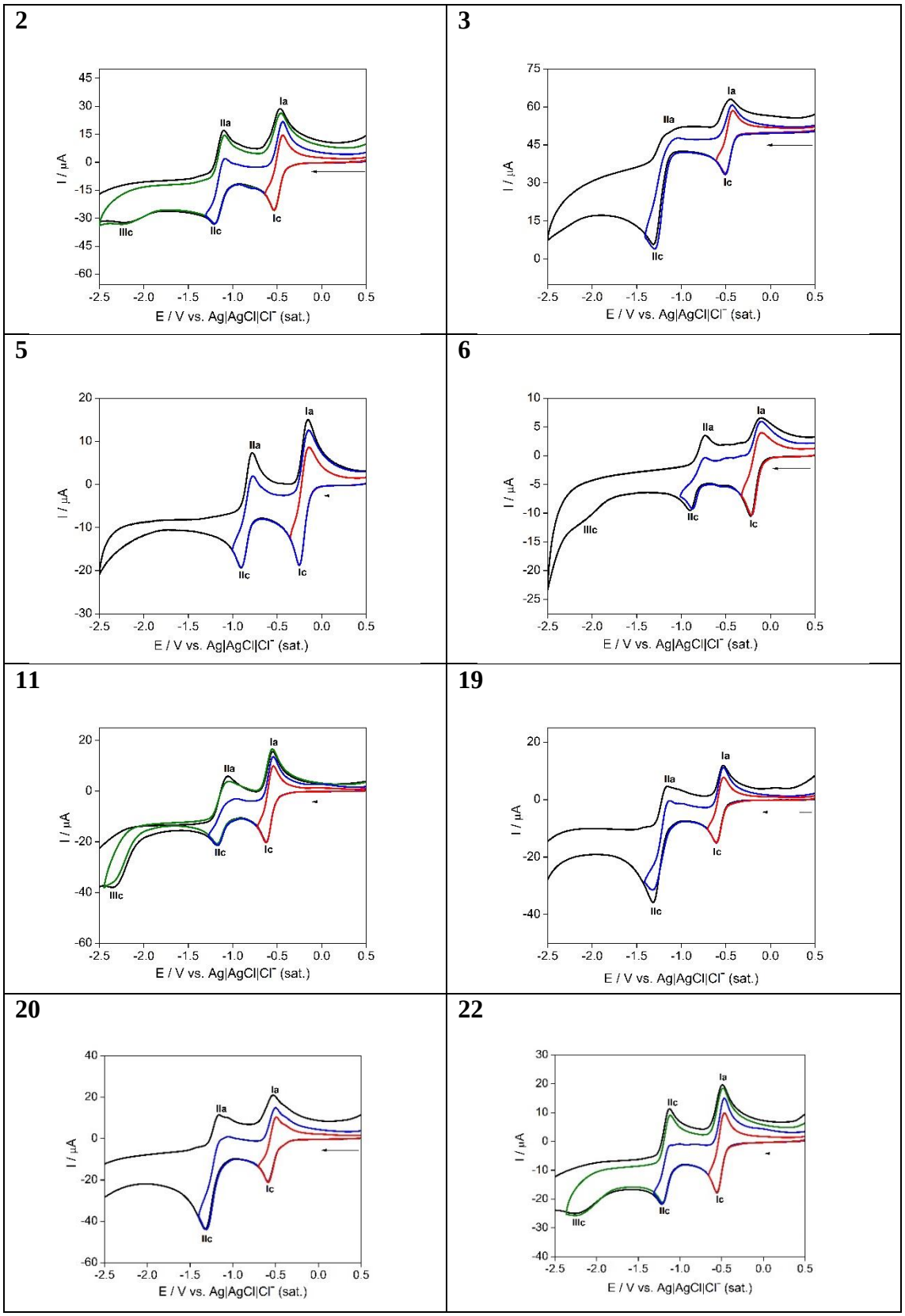

Figure 2. Several inversion potentials in the CV of iodinated quinones **2**, **3**, **5**, **6**, **11**, **19**, **20** and **22** (1 mM) in DMF + $TBAPF_6$ (0.1 M), glassy carbon electrode, cathodic direction, potential range: 0.5 V up to –2.5 V, ν = 0.1 V s^{-1}.

3. Conclusions

The present work shows how a complementary combination of chemical, biological and electrochemical approaches can be used for the identification of new lead compounds for the treatment of Chagas disease. We have described potent trypanocidal naphthoquinones prepared in high efficiency by versatile synthetic methods. Compound **59**, which was prepared in just two steps, has an IC_{50}/24h = 0.19 μM (fifty fold more active than benznidazole) and SI = 62.5 and is thus an important starting point for the development of a new drug against *T. cruzi*. In broader terms, the present study provides an efficient framework to prepare quinoidal compounds with potent activity against the etiological agent of Chagas disease.

4. Experimental Section

4.1. Chemistry

4.1.1. General procedures

1,4-Naphthoquinone and 1,4-benzoquinone were purchased from Alfa Aesar and Sigma Aldrich, purified via reduced pressure sublimation using a cold finger sublimation apparatus (50 °C, 0.9 mbar) and stored in a glovebox to prevent contact with moisture. All commercially available naphthoquinones, benzoquinones and further commercial chemicals were purchased from Sigma Aldrich, Alfa Aesar, Strem Chemicals and Santa Cruz Biotechnology. $[RhCp^tCl_2]_2$ was purchased from Sigma Aldrich.

Substrates **9** and **10**, as well as derivatives **13** and **14** were obtained by reaction with iodomethane and Ag_2O in $CHCl_3$ [17]. Substrates **17** and **18** obtained by oxidation of corresponding tetralones with 2-iodobenzoic acid and Oxone [18]. Substrate **24** was synthesized by nitration of 1,4-naphthoquinone followed by reduction with $SnCl_2/FeCl_3$ [33]. Substrate **27** was synthesised following our latest report [16]. 2,3-Dimethyl-1,4-benzoquinone (**46**), 2-methoxy-1,4-benzoquinone (**47**) and 2,6-dimethoxy-1,4-benzoquinone (**48**) were prepared by oxidation of the corresponding hydroquinones (in case of 2,3-dimethyl-1,4-benzoquinone, the hydroxyl groups of the hydroquinone were methylated with dimethyl sulfate) with silica supported cerium ammonium nitrate [34]. 2,3-Dichloro-1,4-benzoquinone (**52**) was obtained by reaction of 1,4-benzoquinone (**35**) with $SOCl_2/H_2SO_4$ followed by dehydrogenation with Ag_2O [35].

Starting materials available from commercial suppliers were used as received, unless otherwise stated. All reagents requiring purification were purified using standard laboratory techniques, according to methods published by Perrin, Armarego, and Perrin (Pergamon Press, 1966). Catalytic reactions were run under an atmosphere of dry nitrogen or argon; glassware, syringes and needles were either flame dried immediately prior to use or placed in an oven (200 °C), for at least 2 h, and allowed to cool either in a desiccator or under an atmosphere of nitrogen or argon; liquid reagents, solutions or solvents were added via syringe through rubber septa; solid reagents were added inside a glovebox. Melting points were obtained on a Thomas Hoover apparatus and are uncorrected. Column chromatography was performed on silica gel (SiliaFlash G60 UltraPure 60-200 µm, 60 Å). Infrared spectra were recorded on an FTIR Spectrometer IR Prestige-21-Shimadzu. ^{1}H and ^{13}C NMR were recorded at room temperature using a Bruker AVANCE DRX200 and DRX400 MHz instrument, in the solvents indicated. Chemical shifts (δ) are given in parts per million (ppm) and coupling constants (J) in Hertz (Hz). All assignments of NMR spectra were based on 2D NMR data (DEPT-135, COSY, HSQC and HMBC). Mass spectra were recorded using a Brüker Daltonics FT-ICRMS Apex 4e 7.0T FT-MS (ESI^+ mode) and Shimadzu GCMS QP2010+ (EI^+ mode). Infrared spectra were recorded on a Perkin Elmer Spectrum One FTIR spectrometer as thin films or solids compressed on a diamond plate. Data were processed employing Bruker Data Analysis software version 4.0. Compounds were named following IUPAC rules as applied by ChemBioDraw Ultra (version 12.0).

4.1.2. 5-Hydroxy-6-iodo-1,4-naphthoquinone (5). Yield: 88%; m.p. (°C) = 179.8-180.1; red crystals. IR (solid, cm^{-1}) v: 3021 (w), 1698 (s), 1270 (m), 830 (m); HRMS (EI^+): 299.9280 $[M]^+$. Cald. for $[C_{10}H_5IO_3]$: 299.9283; ^{1}H NMR (400 MHz, $CDCl_3$) δ: 12.73 (s, O-H), 8.15 (d, J = 8.0 Hz, C6-H), 7.33 (d, J = 8.0 Hz, C5-H), 6.96 (s, C2-H,C3-H); ^{13}C NMR (100 MHz, $CDCl_3$) δ: 190.0 (C4), 183.8 (C1), 160.1 (C5), 146.1 (C7), 139.8 (C3), 138.0 (C2), 131.5 (C8a), 120.1 (C8), 114.2 (C4a), 94.9 (C6-I).

4.1.3. 5-Hydroxy-6,8-diiodo1,4-naphthoquinone (6). Yield: 82%; m.p. (°C) = 164.3-165.8; purple crystals. IR (solid, cm^{-1}) v: 3002 (w), 1613 (s), 1211 (m), 911 (m); HRMS (EI^+): 425.8241 $[M]^+$. Cald. for $[C_{10}H_4I_2O_3]$: 425.8250; ^{1}H NMR (500 MHz, $CDCl_3$) δ: 13.54 (s, O-H), 8.80 (s, C7-H), 7.04 (d, J = 10.2 Hz, C2-H), 6.96 (d, J = 10.2 Hz, C3-H); ^{13}C NMR (125 MHz, $CDCl_3$) δ: 189.2 (C4), 182.0 (C1), 161.7 (C5), 158.5 (C7), 140.4 (C2), 136.5 (C3), 130.0 (C8a), 115.8 (C4a), 96.0 (C6-I), 83.0 (C8-I).

4.1.4. 5-Hydroxy-6-iodo-2-methyl-1,4-naphthoquinone (8). Yield: 85%; m.p. (°C) = 125.1-125.9; red crystals. IR (solid, cm^{-1}) *v*: 3048 (w), 1687 (s), 1198 (m), 854 (m); MS (EI^+): 313.9 $[M]^+$. Cald. for $[C_{11}H_7IO_3]$: 313.9; ^1H NMR (400 MHz, $CDCl_3$) *δ*: 12.82 (s, 1H), 8.11 (d, *J* = 7.9 Hz, C7-H), 7.35 (d, *J* = 7.9 Hz, C8-H), 6.81 (s, C3-H), 2.19 (s, C9-H_3). ^{13}C NMR (100 MHz, $CDCl_3$) *δ*: 189.9 (C4), 184.3 (C1), 159.9 (C5-OH), 150.0 (C2), 145.6 (C7), 134.8 (C3), 131.9 (C8a), 120.3 (C8), 114.4(C4a), 94.4 C6-I, 16.5 (C9).

4.1.5. 6-Iodo-5-methoxy-1,4-naphthoquinone (13). Yield: 91%; m.p. (°C) = 152.3-152.8; yellow powder. IR (solid, cm^{-1}) *v*: 3014 (w), 1699 (s), 1199 (m), 867 (m); MS (EI^+): 313.9 $[M]^+$. Cald. for $[C_{11}H_7IO_3]$: 313.9; ^1H NMR (400 MHz, $CDCl_3$) *δ*: 8.24 (d, *J* = 8.2 Hz, C7-H), 7.65 (d, *J* = 8.2 Hz, C8-H), 6.95 (d, *J* = 10.3 Hz, C2-H), 6.90 (d, *J* = 10.3 Hz, C3-H), 3.93 (s, C9-H_3). ^{13}C NMR (100 MHz, $CDCl_3$) *δ*: 184.4 (C1), 183.3 (C4), 159.2 (C5), 144.7 (C7), 139.9 (C3), 136.9 (C2), 134.1 (C8a), 124.2 (C8), 124.1 (C4a), 104.2 (C6-I), 61.8 (C9).

4.1.6. 6-Iodo-5-methoxy-2-methyl-1,4-naphthoquinone (14). Yield: 92%; m.p. (°C) = 117.3-118.1; yellow powder. IR (solid, cm^{-1}) *v*: 2985 (w), 1689 (s), 1321 (m), 902 (m); MS (EI^+): 327.9 $[M]^+$. Cald. for $[C_{12}H_9IO_3]$: 327.9; ^1H NMR (400 MHz, $CDCl_3$) *δ*: 8.19 (d, *J* = 8.2 Hz, C7-H), 7.65 (d, *J* = 8.2 Hz, C8-H), 6.76 (s, C3-H), 3.91 (s, C10-H_3), 2.17 (s, C9-H_3).). ^{13}C NMR (100 MHz, $CDCl_3$) *δ*: 185.0 (C1), 183.3 (C4), 158.9 (C5), 146.3 (C2), 144.3 (C7), 136.9 (C3), 134.4 (C8a), 124.4 (C8), 124.3 (C4a), 103.8 (C6-I), 61.8 (C10), 15.9 (C9).

4.1.7. 5-Amino-6-iodo-1,4-naphthoquinone (25). Yield: 41%; m.p. (°C) = 181.2-182.9, purple powder. IR (solid, cm^{-1}) *v*: 3078 (w), 1720 (s), 1380 (m), 923 (m); HRMS (EI^+): 298.9433 $[M]^+$. Cald. for $[C_{10}H_6INO_2]$: 298.9443; ^1H NMR (400 MHz, $CDCl_3$) *δ*: 8.03 (d, *J* = 8.0 Hz, C7-H), 7.15 (d, *J* = 8.0 Hz, C8-H), 6.90 (d, *J* = 10.3 Hz, C3-H), 6.86 (d, *J* = 10.3 Hz, C2-H); ^{13}C NMR (100 MHz, $CDCl_3$) *δ*: 186.65 (C4), 184.97 (C1), 149.21 (C5), 144.79 (C7), 140.05 (C3), 137.20 (C2), 132.92 (C8a), 117.45 (C8), 111.89 (C4a), 95.06 (C6-I).

4.1.8. 2,6-Diiodo-3,5-dimethoxy-1,4-benzoquinone (51). Yield: 91%; m.p. (°C) = 160.2-160.9; red crystals. IR (solid, cm^{-1}) *v*: 2947 (w), 1667 (s), 1266 (s), 924 (s); HRMS (EI^+): 261.9493 $[M]^+$. Cald. for $[C_8H_6I_2O_4]$: 419.8355; ^1H NMR (500 MHz, $CDCl_3$) *δ*: 4.16 (s, C7-H_6); ^{13}C NMR (125 MHz, $CDCl_3$) *δ*: 175.2 (C1), 171.2 (C4), 160.4 (C2,C6), 98.1 (C3,C5), 61.6 (C7).

4.1.9. (*E*)-5-Styrylnaphthalene-1,4-dione (59). Yield: 51%; m.p.(°C): 140.8-141.9; red solid. IR (solid, cm^{-1}) *v*: 2956 (w), 1717 (s), 1632 (s), 1278 (m), 1100 (m), 790

(m); HRMS(EI$^+$): 260.0822. Cald. for $[C_{18}H_{12}O_2]^+$: 260.0837; ^{1}H NMR (500 MHz, $CDCl_3$) δ: 8.30 (d, J = 16.1 Hz, C9-H), 8.10 (dt, J = 7.6, 1.2 Hz, C8-H), 7.98 (dd, J = 7.9, 0.8 Hz, C6-H), 7.72 (t, J = 7.8 Hz, C7-H), 7.62 – 7.60 (m, 2H), 7.43 – 7.37 (m, 2H), 7.35 – 7.29 (m, 1H), 7.06 (d, J = 16.2 Hz, C10-H), 6.95 (d, J = 1.0 Hz,C2-H, C3-H). ^{13}C NMR (125 MHz, $CDCl_3$) δ: 187.0 (C4), 185.2 (C1), 140.5 (C2), 140.2 (C5), 137.1 (C8a), 136.9 (C3), 133.5 (C10), 133.5 (C6), 133.3 (C7), 128.8 (C13, C15), 128.3 (C14), 127.9 (C4a), 127.7 (C9), 127.1 (C12, C16), 126.5 (C8).

4.2. Crystallographic data

X-ray diffraction data collection for three compounds were performed on an Enraf-Nonius Kappa-CCD diffractometer (95 mm CCD camera on κ-goniostat) using graphite monochromated MoK_radiation (0.71073 Å), at room temperature. Data collection was carried out using the COLLECT software [36] up to 50° in 2θ. Integration and scaling of the reflections, correction for Lorentz and polarization effects were performed with the HKL DENZO-SCALEPACK system of programs [37]. The structure of the compounds was solved by direct methods with SHELXS-97 [38]. The models were refined by full-matrix least squares on F^2 using the SHELXL-97 [39]. The program ORTEP-3 [40] was used for graphic representation and the program WINGX [41] to prepare materials for publication. All H atoms were located by geometric considerations (C-H = 0.93-0.97; O-H = 0.82 Å) and refined as riding with Uiso(H) = 1.5Ueq(C-methyl) or 1.2Ueq(other). Crystallographic data for the structures were deposited in the Cambridge Crystallographic Data Centre, with numbers CCDC 1526294, 1526293 and 1526364.

4.3. Animals

Albino Swiss mice were employed for the trypanocidal and cytotoxicity assays, in accordance to the guidelines of the Colégio Brasileiro de Experimentação Animal (COBEA), and these were performed under biosafety conditions. All animal experimentation procedures were approved by the Comissão de Ética em Experimentação Animal (CEUA/Fiocruz), license LW 16/13.

4.4. Trypanocidal Assay

The experiments were performed with the Y strain of *T. cruzi* [42]. Stock solutions of the compounds were prepared in dimethylsulfoxide (DMSO), with the final concentration of the latter in the experiments never exceeding 0.1%. Preliminary experiments showed that at concentrations of up to 0.5%, DMSO has no deleterious effect on the parasites [43]. Bloodstream trypomastigotes were obtained from infected Albino Swiss mice at the peak of parasitemia by differential centrifugation. The parasites were resuspended to a concentration of $10x10^6$ cells/mL in DMES medium. This suspension (100 µL) was added to the same volume of each of the compounds, which had been previously prepared at twice the desired final concentrations. The incubation was performed in 96-well microplates (Nunc Inc., Rochester, USA) at 37°C for 24 h. Benznidazole (Lafepe, Brazil), the standard drug for treatment of chagasic patients, was used as control. Cell counts were performed in a Neubauer chamber, and the activity of the compounds corresponding to the concentration that led to 50% lysis of the parasites was expressed as the IC_{50}/24 h.

4.5. Cytotoxicity to mammalian cells

The cytotoxicity assays were performed using primary cultures of peritoneal macrophages obtained from Albino Swiss mice. For the experiments, $2.5x10^4$ cells in 200 µL of RPMI-1640 medium (pH 7.2 plus 10% foetal bovine serum and 2 mM glutamine) were added to each well of a 96-well microtiter plate and incubated for 24 h at 37°C. The treatment of the cultures was performed in fresh supplemented medium (200 µL/well) for 24 h at 37°C. After this period, 110 µL of the medium was discarded and 10 µL of PrestoBlue (Invitrogen) was added to complete the final volume of 100 µL. Thus, the plate was incubated for 2 h and the measurement was performed at 560 and 590 nm, as recommended by the manufacturer. The results were expressed as the difference in the percentage of reduction between treated and untreated cells being the LC50 value, corresponding to the concentration that leads to damage of 50% of the mammalian cells [25].

4.6. Electrochemical studies

Cyclic voltammetry (CV) experiments were performed with a conventional three electrode cell in an Autolab PGSTAT-30 potentiostat (Echo Chemie, Utrecht, the Netherlands) coupled to a PC microcomputer, using GPES 4.9 software. The working electrode was a glassy carbon (GC) BAS (d = 3 mm), the counter electrode was a Pt wire and the reference electrode an Ag|AgCl, Cl^- (saturated), all contained in a one-compartment electrochemical cell with a volumetric capacity of 5 mL. The GC electrode was cleaned up by polishing with alumina on a polishing felt (BAS polishing kit). The solvent used in aprotic media studies was extra dry N,N-dimethylformamide (99.8%) acquired from Acros Organics. In CV experiments, the scan rate varied from 10 to 1000 mV s^{-1}. Electrochemical reduction and oxidation were performed in aprotic media (DMF + $TBAPF_6$ 0.1 mol L^{-1}) at room temperature (25 ± 2 °C). Each compound (1 x 10^{-3} mol L^{-1}) was added to the supporting electrolyte and the solution was deoxygenated with argon before the measurements by cyclic voltammetry, in different potential intervals.

Appendix A. Supplementary data

Supplementary data related to this article can be found at DOI

Notes

The authors declare no competing financial interest.

Acknowledgements

This research was funded by grants from CNPq (PVE 401193/2014-4, PQ 305385/2014-3, Universal/CNPq 474797/2013-9 and PQ SR Proc. 302613/2013-7), Chamada Universal MCTI/CNPq Nº 01/2016, Fundação Oswaldo Cruz, FAPERJ (CNE Proc. E-26/203.083/2016), FAPEMIG (Edital 01/2014 APQ-02478-14 and Programa Pesquisador Mineiro), FAPEAL and CAPES/PROCAD (88881.068501/2014). J.F.B. is indebted to the Royal Society for a University Research Fellowship. E.N.S.J. also thanks the Royal Society of Chemistry for a JWT Jones Travelling Fellowship.

References

[1] WHO, The Weekly Epidemiological Record, 90 (2015) 33.

[2] (a) M. Steindel, K.L. Pacheco, D. Scholl, M. Soares, M.H. de Moraes, I. Eger, C. Kosman, T.C. Sincero, P.H. Stoco, S.M. Murta, C.J. de Carvalho-Pinto, E.C. Grisard, Diagn. Microbiol. Infect. Dis. 60 (2008) 25;

(b) J.D. Altclas, L. Barcan, C. Nagel, R. Lattes, A. Riarte, JAMA 299 (2008) 34;

(c) J.C.P. Dias, A.V. Neto, Rev. Soc. Bras. Med. Trop. 44 (2011) 68.

[3] (a) WHO, Expert Committee. Control of Chagas Disease. Brasilia Brazil: World Health Organization, WHO technical report series, (2002) 905;

(b) J.C.P. Dias, Epidemiol. Serv. Saúde 25 (2016) 7.

[4] (a) M.A. Shikanai-Yasuda, N.B. Carvalho, Clin. Infect. Dis. 54 (2012) 845;

(b) J.R. Coura, A.C. Junqueira, Acta Trop. 151 (2015) 51.

[5] (a) G.A. Schmunis, Z.E. Yadon, Acta Trop. 115 (2010) 14;

(b) Y. Jackson, V.M. Herrera, J. Gascon, Bull. World Health Organ. 92 (2014) 771.

[6] (a) J.R. Coura, S.L. de Castro, Mem. Inst. Oswaldo Cruz 97 (2002) 3;

(b) K. Salomão, S.L. de Castro, Recent advances in drug development for Chagas disease: two magic words, combination and repositioning. In: Different Aspects on Chemotherapy of Trypanosomatids, Nova Science Publishers, NY, in press.

[7] (a) M.J. Pinazo, J. Munoz, E. Posada, P. López-Chejade, M. Gállego, E. Ayala, E. del Cacho, D. Soy, J. Gascon, Antimicrob. Agents Chemother. 54 (2010) 4896.

(b) Y. Jackson, E. Alirol, L. Getaz, H. Wolff, C. Combescure, F. Chappuis, Clin. Infect. Dis. 51 (2010) 69;

(c) J. Pérez-Molina, F. Norman, R. López-Vélez, Curr. Infect. Dis. Rep. 14 (2012) 263;

[8] K. Salomão, R.F. Menna-Barreto, S.L. de Castro, Curr. Top. Med. Chem. 16 (2016) 2266.

[9] (a) S.B.B.B. Bahia, W.J. Reis, G.A.M. Jardim, F.T. Souto, C.A. de Simone, C.C. Gatto, R.F.S. Menna-Barreto, S.L. de Castro, B.C. Cavalcanti, C. Pessoa, M.H. Araujo, E.N. da Silva Júnior, Med. Chem. Commun. 7 (2016) 1555;

(b) T. Kumar, D. Verma, R.F.S. Menna-Barreto, W.O. Valença, E.N. da Silva Júnior, I.N. N. Namboothiri, Org. Biomol. Chem. 13 (2015) 1996;

(c) S.L. de Castro, F.S. Emery, E.N. da Silva Júnior, Eur. J. Med. Chem. 69 (2013)

678;

(d) E.N. da Silva Junior, G.A.M. Jardim, R.F.S. Menna-Barreto, S.L. de Castro, J. Braz. Chem. Soc. 25 (2014) 1780.

[10] C. Neves-Pinto, V.R.S. Malta, M.C.F.R. Pinto, R.H.A. Santos, S.L. de Castro, A.V. Pinto, J. Med. Chem. 45 (2002) 2112.

[11] E.N. da Silva Junior, T.T. Guimaraes, R.F.S. Menna-Barreto, M.C.F.R. Pinto, C.A. de Simone, C. Pessoa, B.C. Cavalcanti, J.R. Sabino, C.K.Z. Andrade, M.O.F. Goulart, S.L. de Castro, A.V. Pinto, Bioorg. Med. Chem. 18 (2010) 3224.

[12] S.M. Lim,Y. Jeong, S. Lee, H. Im, T.H. Seop, B.G. Kim, H.D. Park, J. Park, S. Hong, J. Med. Chem. 58 (2015) 8491.

[13] (a) K. Salomão, N.A. Santana, M. T. Molina, S. L. de Castro, R. F. S. Menna-Barreto, BMC Microbiol. 13 (2013) 196;

(b) E.O. Costa, M.T. Molina, F.C. Abreu, F.A.S. Silva, C.O. Costa, W. Pinho Júnior, I.B. Valentim, B. Aguilera-Venegas, F. Pérez-Cruz, E. Norambuena, C. Olea-Azar, M.O.F. Goulart, Int. J. Electrochem. Sci. 7 (2012) 6524.

[14] D.K. Nair, R.F.S. Menna-Barreto, E.N. da Silva Júnior, S.M. Mobin, I.N.N. Namboothiri, Chem. Commun. 50 (2014) 6973.

[15] T. Gensch, M.N. Hopkinson, F. Glorius, J. Wencel-Delord, Chem. Soc. Rev. 45 (2016) 2900.

[16] G.A.M. Jardim, E.N. da Silva Júnior, J.F. Bower, Chem. Sci. 7 (2016) 3780.

[17] (a) P.M. Boyer, C.P. Roy, J.M. Bielski, J.S. Merola, Inorg. Chim. Acta 245 (1996) 7;

(b) Y. Bendiabdellah, K.M. Rahman, B. Uranchimeg, K.S. Nahar, D. Antonow, R.H. Shoemaker, G. Melillo, G. Zinzalla, D.E. Thurston, Med. Chem. Commun. 5 (2014) 923.

[18] J. Ren, L. Lu, J. Xu, T. Yu, B. Zeng Synthesis 47 (2015) 2270.

[19] N.V. Ivashkina, E.A. Yakovleva, I.D. Ivanchikova, A.A. Moroz, M.S. Shvartsberg, Russ. Chem. Bull., Int. Ed. 54 (2005) 1509.

[20] G.A.M. Jardim, J.F. Bower, E.N. da Silva Júnior, Org. Lett. 18 (2016) 4454.

[21] S.P.H. Mee, V. Lee, J.E. Baldwin, Angew. Chem. Int. Ed. 43 (2004) 1132.

[22] P.M. Murray, J.F. Bower, D.K. Cox, E.K. Galbraith, J.S. Parker, J.B. Sweeney, Org. Process Res. Dev. 17 (2013), 397.

[23] N.V. Ivashkina, V.S. Romanov, A.A. Moroz, M.S. Shvartsberg, Russ. Chem. B. 33 (1984) 2345.

[24] A.O. da Silva, R.S. Lopes, R.V. de Lima, C.S.S. Tozatti, M.R. Marques, S. de Albuquerque, A. Beatriz, D.P. de Lima, Eur. J. Med. Chem. 60 (2013) 51.

[25] C.O. Ogindo, M.H. Khraiwesh, M. George Júnior, Y. Brandy, N. Brandy, A. Gugssa, M. Ashraf, M. Abbas, W.M. Southerland, C.M. Lee, O. Bakare, Y. Fang, Bioorg. Med. Chem. 24 (2016) 3849.

[26] (a) F.C. de Abreu, P.A.L. Ferraz, M.O.F. Goulart, J. Braz. Chem. Soc. 13 (2002) 19; (b) Y.G. de Paiva, F.R. Ferreira, T.L. Silva, E. Labbe, O. Buriez, C. Amatore, M.O.F. Goulart, Curr. Top. Med. Chem. 15 (2015) 136.

[27] (a) A.J. Araújo, A.A. de Souza, E.N. da Silva Júnior, J.D.B. Marinho-Filho, M.A.B.F. de Moura, D.D. Rocha, M.C. Vasconcellos, C.O. Costa, C. Pessoa, M.O. de Moraes, V.F. Ferreira, F.C. de Abreu, A.V. Pinto, R.C. Montenegro, L.V. Costa-Lotufo, M.O.F. Goulart, Toxicol. in Vitro 26 (2012) 585;

(b) G. Armendáriz-Vidales, L.S. Hernández-Muñoz, F.J. González, A.A. de Souza, F.C. de Abreu, G.A.M. Jardim, E.N. da Silva Júnior, M.O.F. Goulart, C. Frontana, J. Org. Chem. 79 (2014) 5201.

[28] G.A.M. Jardim, W.J. Reis, M.F. Ribeiro, F.M. Ottoni, R.J. Alves, T.L. Silva, M.O.F. Goulart, A.L. Braga, R.F.S. Menna-Barreto, K. Salomão, S.L. de Castro, E.N. da Silva Júnior, RSC Adv. 5 (2015) 78047.

[29] (a) E.H.G. da Cruz, C.M.B. Hussene, G.G. Dias, E.B.T. Diogo, I.M.M. de Melo, B.L. Rodrigues, M.G. da Silva, W.O. Valença, C.A. Camara, R.N. de Oliveira, Y.G. de Paiva, M.O.F. Goulart, B.C. Cavalcanti, C. Pessoa, E.N. da Silva Júnior, Bioorg. Med. Chem. 22 (2014) 1608. (b) J.S. Walsh, G.T. Miwa, Annu. Rev. Pharmacol. Toxicol. 51 (2011) 145.

[30] P. Sanecki, Computers Chem. 25 (2001) 521.

[31] E.A. Hillard, F.C. de Abreu, D.C.M. Ferreira, G. Jaouen, M.O.F. Goulart, C. Amatore, Chem. Commun. 23 (2008) 2612.

[32] (a) J.M. Saveant, Elements of Molecular and Biomolecular Electrochemistry, Wiley, New York, 2006;

(b) C.P. Andrieux, A. Le Gorande, J.M. Saveant, J. Am. Chem. Soc. 114 (1992) 6892;

(c) A. Gennaro, A.A. Isse, C.L. Bianchi, P.R. Mussini, M. Rossi, Electrochem. Commun. 11 (2009) 1932.

[33] N.V. Ivashkina, V.S. Romanov, A.A Moroz, M.S. Shvartsberg, Russ. Chem. Bull. 33 (1984) 2345.

[34] M.H. Ali, M. Niedbalski, G. Bohnert, D. Bryant, Synth. Commun. 36 (2006) 1751.

[35] I. Pochorovski, C. Boudon, J.P. Gisselbrecht, M.O. Ebert, W.B. Schweizer, F. Diederich, Angew. Chem. Int. Ed. 51 (2012) 262.

[36] B.V. Nonius, Enraf-Nonius COLLECT Delft, The Netherlands, (1997-2000).

[37] Z. Otwinowski, W. Minor, C.W. Carter, R.M. Sweet, Methods in Enzymology, vol. 276, Academic Press, New York, (1997) 307.

[38] G.M. Sheldrick, SHELXS-97. Program for Crystal Structure Resolution. University of Göttingen, Göttingen, Germany, (1997).

[39] G.M. Sheldrick, SHELXL-97. Program for Crystal Structure Refinement. University of Göttingen, Göttingen, Germany, (1997).

[40] L.J. Farrugia, J. Appl. Crystallogr. 30 (1997) 565.

[41] L.J. Farrugia, J. Appl. Crystallogr. 32 (1997) 837.

[42] L.H.P. Silva, V. Nussenszweig, Folia Clin. Biol. 20 (1953) 191.

[43] S.L. de Castro, M.C.F.R. Pinto, A.V. Pinto, Microbios 78 (1994) 83.